Quantitative measurement of binocular color fusion limit for non-spectral colors

Yong Ju Jung, Hosik Sohn, Seong-il Lee, Yong Man Ro,* and Hyun Wook Park

Department of Electrical Engineering, Korea Advanced Institute of Science and Technology, Daejeon 305-701, Korea

*ymro@ee.kaist.ac.kr

Abstract: Human perception becomes difficult in the event of binocular color fusion when the color difference presented for the left and right eyes exceeds a certain threshold value, known as the binocular color fusion limit. This paper discusses the binocular color fusion limit for non-spectral colors within the color gamut of a conventional LCD 3DTV. We performed experiments to measure the color fusion limit for eight chromaticity points sampled from the CIE 1976 chromaticity diagram. A total of 2480 trials were recorded for a single observer. By analyzing the results, the color fusion limit was quantified by ellipses in the chromaticity diagram. The semi-minor axis of the ellipses ranges from 0.0415 to 0.0923 in terms of the Euclidean distance in the u′v′ chromaticity diagram and the semi-major axis ranges from 0.0640 to 0.1560. These eight ellipses are drawn on the chromaticity diagram.

OCIS codes: (330.1400) Vision – binocular and stereopsis; (330.1720) Color vision; (330.1710) Color, measurement.

References and links

1. M. Lambooij, W. Ijsselsteijn, M. Fortuin, and I. Heynderickx, "Visual discomfort and visual fatigue of stereoscopic displays: a review," J. Imaging Sci. Technol. **53**(3), 1–14 (2009).
2. J. K. Hovis, "Review of dichoptic color mixing," Optom. Vis. Sci. **66**(3), 181–190 (1989).
3. I. P. Howard, *Seeing in depth* (I. Porteous, 2002), Chap. 7.
4. M. Ikeda, and K. Sagawa, "Binocular color fusion limit," J. Opt. Soc. Am. **69**(2), 316–320 (1979).
5. M. Ikeda, and Y. Nakashima, "Wavelength difference limit for binocular color fusion," Vision Res. **20**(8), 693–697 (1980).
6. H. Ujike, et al., "ISO International Workshop Agreement-IWA3 Image Safety - reducing the incidence of undesirable biomedical effects caused by visual image sequences. IWA 3:2005(E), " (ISO copyright office, Case postale 56, CH-1211 Geneva 20, 2005).
7. C. Shigeru, "3D consortium safety guidelines for popularization of human-friendly 3D," Tech. Rep. 3D Consortium (Japan, 1996).
8. Q. Huynh-Thu, P. L. Callet, and M. Barkowsky, "Video quality assessment: from 2D to 3D - challenges and future trends," in *Proceedings of IEEE International Conference on Image Processing* (Institute of Electrical and Electronics Engineers, New York, 2010), pp. 4025–4028.
9. D. L. Macadam, "Visual sensitivities to color differences in daylight," J. Opt. Soc. Am. **32**(5), 247–274 (1942).
10. D. Qin, M. Takamatsu, Y. Nakashima, and X. Qin, "Change of wavelength difference limit for binocular color fusion with wavelength and brightness of stimuli," J. Light Vis. Environ. **30**(1), 43–45 (2006).
11. W. D. Wright, "The sensitivity of the eye to small colour differences," Proc. Phys. Soc. **53**(2), 93–112 (1941).
12. E. F. Schubert, *Light-emitting diodes* (Cambridge Univ. Press, 2006), Chap. 17.
13. G. Verriest, J. Van Laethem, and A. Uvijls, "A new assessment of the normal ranges of the Farnsworth-Munsell 100-hue test scores," Am. J. Ophthalmol. **93**(5), 635–642 (1982).
14. A. Woods, "Understanding crosstalk in stereoscopic displays," presented in Keynote Presentation at the Three-Dimensional Systems and Applications Conference, Tokyo, Japan, 19–21 May 2010.
15. J.-C. Liou, K. Lee, F.-G. Tseng, J.-F. Huang, W.-T. Yen, and W.-L. Hsu, "Sutter glasses stereo LCD with a dynamic backlight," Proc. SPIE **7237**, 72370X, 72370X-8 (2009).
16. G. Sharma, "LCDs versus CRTs - color-calibration and gamut considerations," Proc. IEEE **90**(4), 605–622 (2002).
17. Y.-K. Cheng, and H.-P. D. Shieh, "Colorimetric characterization of high dynamic range liquid crystal displays and its application," J. Display Technol. **5**(1), 40–45 (2009).
18. P. L. Rosin, "Fitting superellipses," IEEE Trans. Pattern Anal. Mach. Intell. **22**(7), 726–732 (2000).
19. A. S. H. Ler, M. A. Cohen, and J. A. Taylor, "A planar elliptical model of cardio-vagal hysteresis," Physiol. Meas. **31**(6), 857–873 (2010).

#140993 - $15.00 USD Received 12 Jan 2011; revised 10 Mar 2011; accepted 21 Mar 2011; published 1 Apr 2011

20. ITU-R BT-500, 11, "Methodology for the subjective assessment of the quality of television pictures," International Telecommunications Union (2002).

1. Introduction

Starting with the recent success of the stereoscopic three-dimensional (3D) cinema industry, stereoscopic 3D content services are the subject of great interest from many industries, including the 3D broadcasting industry. However, one of the main bottlenecks preventing the proliferation of stereoscopic 3D services into the mass market is the concern over visual fatigue and visual discomfort that can be induced at various stages, including stereo shooting and 3D production, coding and transmission, and rendering on stereoscopic displays [1].

In stereopsis, binocular asymmetry may be one of the causes of visual fatigue and visual discomfort. Human perception becomes difficult in the event of binocular fusion when the level of asymmetries exceeds a certain limit [2,3]. There are three categories of the binocular asymmetries: luminance asymmetry, chromaticity asymmetry, and structure asymmetry [4]. Specifically, nonfused impressions in dichoptic color viewing have been reported as color rivalry or superimposition [2]. Color rivalry is a periodic alternation of the image in each eye occurring in either the spatial or temporal domain. Superimposition appears as simultaneous perception of both colors.

There is a great need to investigate and quantitatively determine the chromatic fusion limit in dichoptic viewing. This quantitative fusion limit can be used for various applications to provide users with comfortable viewing, such as an automatic stereo analyzer to guide content creators for the creation of visually comfortable stereoscopic contents, manufacturing guidelines to create safe optical instruments, image safety guidelines for users who watch 3DTV, and automatic content adaptation to reduce the level of visual discomfort [6–8].

Ikeda *et al.* studied the color fusion limits of spectral colors and white light [4,5]. Their experiments were conducted to determine the wavelength difference that initiated color rivalry. The color fusion limit was quantified as a function of the wavelength for the spectral colors. The wavelengths of the stimuli ranged from 500 to 660 nm. Seventeen sample points were subjectively examined to find the color fusion limit. These points were presented for the right eye. In addition, each point for the right eye was coupled with ten neighboring wavelengths for the left eye. The results of the wavelength difference ranged from 10 to 50 nm with a minimum value near 480 nm and 580 nm and a maximum value at the spectral extremes [2]. They also reported the color fusion limit for white point as a circle with a radius of about 0.0792 in the CIE 1960 uv chromaticity diagram [4]. However, their works were limited to spectral colors and white light.

As 3DTV has spread, it is necessary to measure how color differences between left and right images of non-spectral colors as well as spectral colors initiate color rivalry. In particular, the color fusion limit of non-spectral colors needs to be measured in the color gamut of 3DTV. Thus far, no attempt has been made to measure the color fusion limit for non-spectral colors.

In this paper, we measure the binocular color fusion limit for non-spectral colors within the color gamut of a conventional LCD (Liquid Cristal Display) 3DTV. The color fusion limit is measured for eight chromaticity points, covering the entire area in the standard CIE 1976 u´v´ chromaticity diagram. In order to check the consistency of our measurements with the results of a previous study, the color fusion limit for a white point was compared to that in a previous study [4]. For eight chromaticity points, *over two thousand trials* were recorded for a single observer. It takes very long time to observe all stimuli, and the long observation time necessary for the asymmetrical visual stimuli can induce visual fatigue such as eye strain. To limit this investigation to reasonable proportions, it was considered that only a single trichromat would cover all eight chromaticity points to complete this investigation. And four selected chromaticity points were tested by an author to confirm the results of the trichromat. The experimental results show the color fusion limit represented in terms of the Euclidean distance along straight lines in the chromaticity diagram. We quantify the color fusion limit of each point through the use of ellipses, as shown in the color differences obtained by

#140993 - $15.00 USD Received 12 Jan 2011; revised 10 Mar 2011; accepted 21 Mar 2011; published 1 Apr 2011

Macadam's experiment [9]. These results were tabulated and then drawn on a standard chromaticity diagram.

The rest of this paper is organized as follows. In section 2, we describe the experimental method used for the measurement of the color fusion limit. Experimental results are presented in section 3, illustrating the color fusion limit plotted in the CIE 1976 uniform chromaticity scale diagram. Finally, section 4 concludes this paper.

2. Method

2.1 Apparatus and test material

The apparatus for the present experiments was a calibrated stereoscopic monitor manufactured by Redrover (true3Di®). It consisted of two 40" TFT-LCD displays by Samsung Electronics (LTA400HA07®) and a half mirror. The stereoscopic 3D monitor exploited the linear polarization technique. The viewers watched stereoscopic stimuli upon wearing polarized glasses. The viewing distance was 1.5m. Figure 1 shows the apparatus used in our experiment. Table 1 summarizes the specifications of the LCD display. The brightness and chromaticity were measured at the center point of the monitor using a spectroradiometer (Minolta CS-1000®). The crosstalk levels of the stereoscopic 3D monitor were 0.75% for the left eye and 0.27% for the right eye [14,15]. Both crosstalk levels were as low as visibility threshold of about 1 to 2%, as reported in previous literature [14].

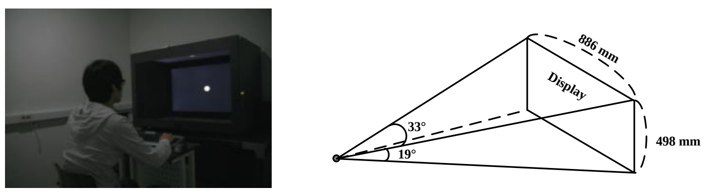

(a) (b)

Fig. 1. (a) Apparatus and (b) viewing environment used in our experiment for the investigation of the color fusion limit.

Table 1. Specifications of LCD Displays Used in Our Experiment. The Brightness and Chromaticity Were Measured at the Center Point of the Monitor With a Spectroradiometer. H and V Respectively Denote the Horizontal and Vertical Size of the Display.

Display area (mm)		Aspect ratio	Resolution	Brightness (with glasses, cd/m^2)	
				left	right
886 (H)	498 (V)	16:9	1920 x 1080	149	136

Pixel arrangement	Display colors	Color gamut	Color chromaticity			
			red	green	blue	white
RGB vertical strip	8bit, 16.7M colors	72% of NTSC	x = 0.642 y = 0.337	x = 0.280 y = 0.605	x = 0.147 y = 0.060	x = 0.280 y = 0.290

we uniformly sampled the points in the CIE 1976 uniform chromaticity scale diagram. Figure 2 shows all eight sample points in the CIE 1976 chromaticity diagram, where we measured the color fusion limit. The numbers in Fig. 2 indicate the sample numbers to be observed for the color fusion limit and the triangle represents the color gamut of the LCD display used in our experiments. In the experiments, the colors of the sampled points were presented for the right eye.

#140993 - $15.00 USD Received 12 Jan 2011; revised 10 Mar 2011; accepted 21 Mar 2011; published 1 Apr 2011

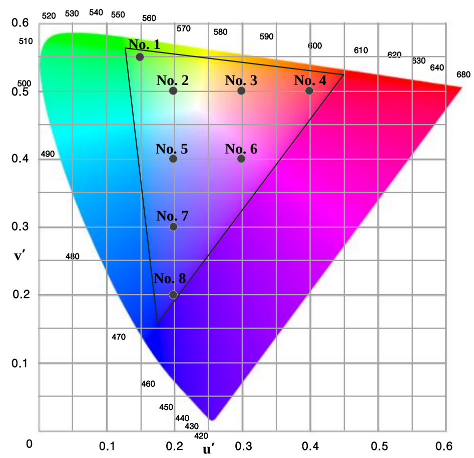

Fig. 2. The total of 8 sample points in the CIE 1976 chromaticity diagram where we quantify color fusion limit through our experiment. The triangle represents the color gamut of the LCD display used in our experiments. The numbers indicate the sample numbers (from No. 1 to No. 8). These sample points were presented for the right eye.

To prepare the stimuli for the left eye, which were coupled with the stimulus given for the right eye, we sampled neighbors along the straight lines of six directions from the origin point given for the right eye. The six directions consisted of:

- Three main directions to the red (R), green (G), and blue (B) primaries.
- Three sub-directions representing an equiangular division between R and G, G and B, and B and R, respectively.

Seven chromaticity points were sampled along each line while uniformly increasing the distance from the origin points for the right eye. Figure 3 illustrates examples of the neighbor selection scheme for the No. 3 and No. 5 points in Fig. 2. The sampling step size is 0.02. Here, the neighbor points were selected from inside of the color gamut of the LCD display. Consequently, the maximum number of neighbor points for each of the eight points for the right eye is 42 (= 6 directions x 7 neighbor points).

We should note that as more samples are examined, more accurate information is obtained to quantify the color fusion limit. In our experiments, however, we compromised regarding the number of stimulus samples to prevent the number of observations from becoming too large for an observer. There were 248 stimuli overall for each of the eight chromaticities: 23 for No. 1, 30 for No. 2, 35 for No. 3, 25 for No. 4, 36 for No. 5, 37 for No. 6, 33 for No. 7, and 29 for No. 8 (see Table 3 and Table 4 in Appendix).

In our experiments, the sample points along each chromaticity vector did not exactly sit on straight lines as shown in Fig. 3. This was mainly due to the LCD monitor calibration. In the conventional LCD color-calibration techniques that exploit gamma correction or tone response correction with look up Tables [16,17], calibrated monitor output included calibration error, which was not negligible for our measurement of the color fusion limit. As such, we utilized a direct measurement method by constructing a mapping table between RGB and tri-stimulus values:

1) We directly measured a set of candidate points in the entire chromaticity diagram. In order to construct the mapping table, first we prepared a set of u'v' values sampled with the step size of 0.005 (i.e., an intended precision of our measurement) in the entire area of the CIE 1976 diagram. Second, the u'v' values (sampled with the step size of 0.005), constrained at a brightness level of 10cd/m^2, were transformed to RGB values using gamma correction functions with the gamma values estimated in our monitor calibration. Third, the transformed RGB values were inputted into the left and right LCD monitors, respectively. Finally, the u'v' chromaticity and

#140993 - $15.00 USD Received 12 Jan 2011; revised 10 Mar 2011; accepted 21 Mar 2011; published 1 Apr 2011

luminance values for each input were measured using a spectroradiometer (Minolta CS-1000®) attached to polarized glasses in front of camera lens. The mapping table between RGB and tri-stimulus values was constructed using the directly measured values. All procedure was automatically performed by a third-party software program.

2) Among the candidate points in the mapping table, we selected the nearest points to the points on straight lines. The nearest points were used for visual stimuli in our experiment. As a result, Table 3 and Table 4 in Appendix show the u', v', and luminance values of all the visual stimuli. The average u'v' difference between the sample points on straight lines and the nearest points in the mapping table was 0.003 in the Euclidean distance. The colorimetric errors were negligible as low as the intended precision (i.e., 0.005) of our measurement for the color fusion limits.

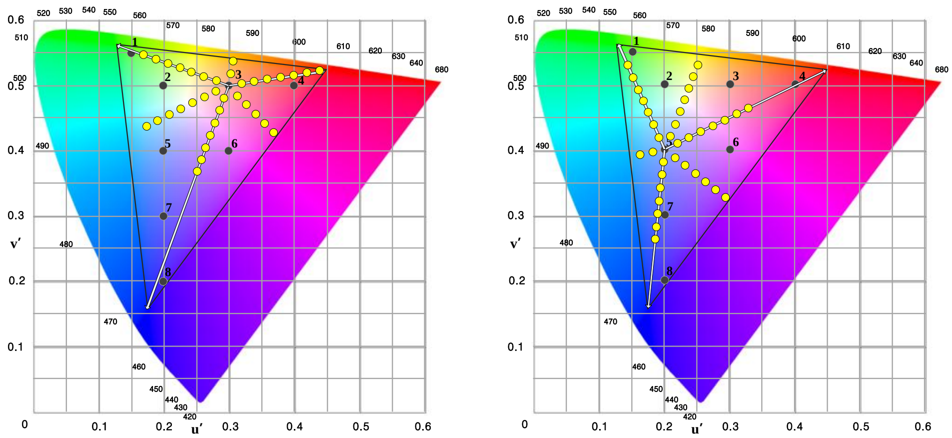

(a) (b)

Fig. 3. Examples of the neighbor selection scheme for the (a) No. 3 and (b) No. 5 sample points illustrated in Fig. 2. The selections were sampled along straight lines in six directions with a uniform step size of 0.02. The triangle represents the color gamut of the LCD display used in our experiments. The colors of the selected neighbor points were presented for the left eye.

(a) (b)

Fig. 4. Example of a stimulus used in the binocular color fusion limit experiment (a) for the left eye and (b) for the right eye. The test field size was 2° in diameter, and the surrounding field size was 33°.

We used a black background and a circular object filled with the sampled colors. The binocular disparity was zero, indicating no depth perception. Figure 4 shows an example of a stimulus. It consists of different colors for the left and right eyes.

In the experiments, the test field size had a visual angle of 2° and a brightness level of 10 cd/m^2. The background intensity was 0.05 cd/m^2 and the viewing duration was 15 seconds. Many studies have been conducted to investigate the characteristics related to the dependency on binocular color fusion and rivalry [3]. Hovis provided a useful review of these

#140993 - $15.00 USD Received 12 Jan 2011; revised 10 Mar 2011; accepted 21 Mar 2011; published 1 Apr 2011

dependencies on binocular color fusion [2]. He concluded that color fusion was more likely to occur with a visual field size smaller than 1°. Ikeda and Sagawa also reported that the fusion increased as the size increased to 45´ and then stayed constant up to 1°20′ [4]. Based on this preliminary observation, they used a 1° visual field size in their experiments on wavelength differences. However, Ikeda and Nakashima pointed out that the variance between observers was not small as a consequence of a small field size, 1° [5]. Thus, they employed larger field sizes of 2° and 10° in their subsequent experiments. From their observations, the wavelength difference values at 2° were somewhat larger than those in a 10° visual field. Color fusion becomes more stable when the absolute luminance of the stimulus is lowered. Qin *et al.* studied the wavelength difference limit with the four brightness levels of 3 cd/m^2, 7.5 cd/m^2, 15 cd/m^2 and 30 cd/m^2 [10]. They showed that the fusion limit becomes smaller as the brightness level increases. Color fusion is more stable with a dark background than with a white background [2]. It is also known that as the viewing duration increases, color fusion becomes more stable. Researchers generally agree that color fusion is more stable with a viewing duration of 3 to 15 seconds [2]. Ikeda and Sagawa also reported that the degree of rivalry increased to 15 seconds and stayed constant up to 25 seconds [4]. From these earlier reports, we designed the experimental parameters for our stimulus.

2.2 Procedure

For the right eye, a sample point was randomly chosen from among the eight sample points depicted in Fig. 2. For the left eye, its neighboring different chromaticity points were presented. An observer was exposed to the stimulus for 15 seconds and reported either fused or nonfused by a forced choice method during a resting time of 10 seconds. After the observations of all neighboring chromaticities were performed, the observations were repeated ten times in a random order [4]. After the ten observations for each pair of the left and right stimuli, the observer chose another sample point for the right eye.

A total of 2480 (= 248 stimuli x 10 observations) trials were recorded for a single observer. The observation process for all of the stimuli was lengthy and induced visual fatigue. Thus, the observations were divided into several test sessions consisting of several 30-min sessions. The observations were stopped immediately when the observer sensed any visual fatigue. The test was conducted under approval from the KAIST Institutional Review Board (IRB).

Based on the results derived from all the observations, the percentage of fused perceptions was calculated for each pair of stimuli. 50 percent of fused perceptions were then used as the color fusion limit [4]. Furthermore, the color fusion limit was quantified as ellipses for the eight sample points in the chromaticity diagram.

3. Results and discussion

The overall results of the observations by a single observer, DH, are presented in Tables 3 and 4 in Appendix. Figure 5 shows three examples of the percentage of fused perceptions, p(%), at the chromaticity point (*u´*=0.15, *v´*=0.55) represented by the No. 1 point in Fig. 2 and Table 3. The abscissa represents the Euclidean distance from the point in the u’v´ chromaticity diagram. Each psychometric function shows the percentages for the neighbors in a line of the direction sampled for the left eye. We selected a 50% fused level as the color fusion limit. As indicated in [4], the fusion points were estimated by using linear interpolation between two adjacent points near the 50% of fused level. The fusion points were calculated as follows:

$$u'_f = u'_i + (u'_{i-1} - u'_i)\frac{50 - p_i}{p_{i-1} - p_i}, \tag{1}$$

$$v'_f = v'_i + (v'_{i-1} - v'_i)\frac{50 - p_i}{p_{i-1} - p_i}, \tag{2}$$

#140993 - $15.00 USD Received 12 Jan 2011; revised 10 Mar 2011; accepted 21 Mar 2011; published 1 Apr 2011

where u'_i and v'_i denote the first chromaticity sample point at the below 50% of fused level, and p_i denotes the percentage of fused perceptions at the point i, and u'_f and v'_f denote the fused chromaticity point for the color fusion limit. For example, p_i=40, p_{i-1}=80, (u'_i=0.2505, v'_i =0.5429), and (u'_{i-1}=0.2307, v'_{i-1}=0.5450) were read out in Fig. 5(a) and Table 3. Using Eq. (1) and Eq. (2), the color fusion limit was computed as (u'_f=0.2456, v'_f=0.5434) for the red direction. Similarly, from the observed psychometric function in Fig. 5(b) and Fig. 5(c), the color fusion limits were interpreted as (u'_f=0.1588, v'_f=0.4727) for the blue direction, and (u'_f=0.2204, v'_f=0.4793) for the blue-red direction. Figure 6 shows another example of the percentage of fused perceptions at the No. 6 point (u'=0.3, v'=0.4). In the same way, the chromaticity points of the color fusion limits were obtained as follows: (u'_f=0.3710, v'_f=0.4585) for the red direction, (u'_f = 0.3057, v'_f = 0.4952) for the red-green direction, (u'_f = 0.2500, v'_f=0.4431) for the green direction, (u'_f=0.2462, v'_f=0.3925) for the green-blue direction, and (u'_f=0.2577, v'_f=0.3170) for the blue direction, respectively.

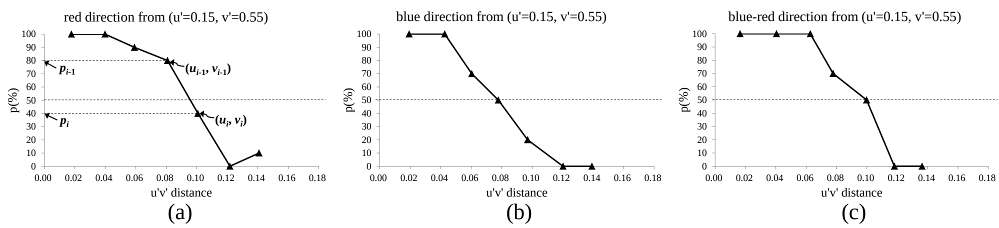

Fig. 5. Percentage of fused perceptions regarding the left stimuli sampled in each neighbor's direction from the No. 1 point (u´=0.15, v´=0.55). The abscissa represents the Euclidean distance from the point (u´=0.15, v´=0.55). p(%) denotes the percentage of fused perceptions. Observer: DH. (a) Red direction, (b) blue direction, and (c) blue-red direction.

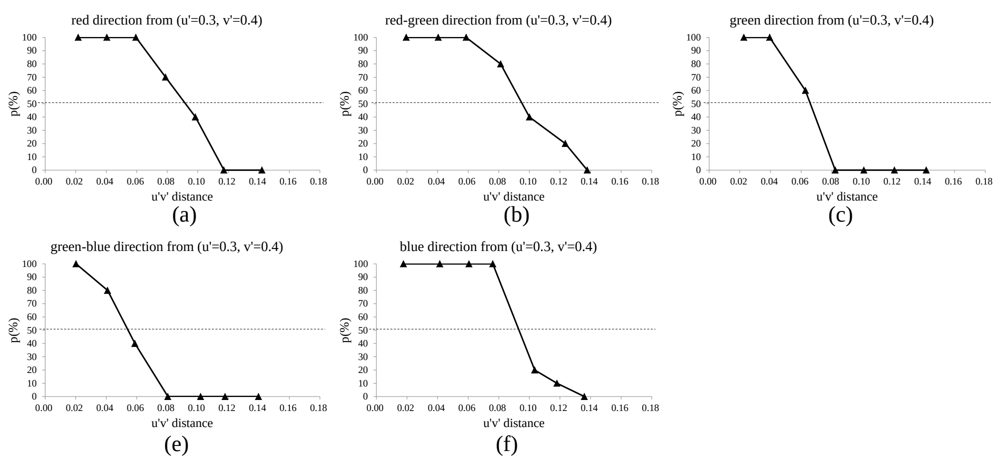

Fig. 6. Percentage of fused perceptions regarding the left stimuli sampled in each neighbor's direction from the No. 6 point (u´=0.3, v´=0.4). Observer: DH. (a) Red direction, (b) red-green direction (c) green direction (d) green-blue direction, and (e) blue direction.

Based on the results of the percentage of fused perceptions, we observed that the shape of the chromaticity points of the color fusion limit could be represented by ellipses. To confirm the shape of the color fusion limit, four additional neighboring directions from the No. 3 point were tested. The four additional directions also represented an equiangular division between the five directions from the No. 3 point. Thus, a total of nine chromaticity points of the color fusion limit were measured for the No. 3 point. For the nine chromaticity points, the sums of square errors in the regression of the ellipse and circle were 0.3912 and 0.4311, respectively.

#140993 - $15.00 USD Received 12 Jan 2011; revised 10 Mar 2011; accepted 21 Mar 2011; published 1 Apr 2011

From the above observations, we modeled the color fusion limit using a set of ellipses [9]. This can be defined as

$$\frac{((u'-C_1)\cos\theta+(v'-C_2)\sin\theta)^2}{a^2}+\frac{(-(u'-C_1)\sin\theta+(v'-C_2)\cos\theta)^2}{b^2}=1, \quad (3)$$

where a and b are the semi-minor and semi-major axes from the center point (C_1, C_2), respectively, and θ is the rotation angle of the ellipse. The parameters of the ellipse were obtained by nonlinear regression. In addition, we examined the goodness-of-fit statistics for the nonlinear regressions: the sum of squares due to error (SSE) and R-squared value referred from [18, 19]. The SSE, also called the residual sum of squares, was measured by the sum of squared algebraic distances as follows:

$$SSE=\sum_{f=1}^{n}\left(\left(\frac{(u_f^{'}-C_1)\cos\theta+(v_f^{'}-C_2)\sin\theta}{a}\right)^2+\left(\frac{-(u_f^{'}-C_1)\sin\theta+(v_f^{'}-C_2)\cos\theta}{b}\right)^2-1\right)^2, \quad (4)$$

where a, b, and θ denote the parameters of the ellipse model, and where $u_f^{'}$ and $v_f^{'}$ denote the fused chromaticity point of the color fusion limit [18]. The fitting of an ellipse was realized by minimizing the sum of squared algebraic distances. As for iterative estimation algorithm, "Levenberg-Marquardt" method was adopted for the purpose of estimating the nonlinear function. The iterations were stopped when a convergence criterion was reached. The convergence criterion used was $1.0e^{-8}$. For the ellipse represented in Fig. 7(a), C_1 was 0.15, C_2 was 0.55, a was 0.0707, b was 0.1049, and θ was 62.0273 degrees, respectively. The standard errors of the regression are 0 for a, 0 for b, and 0.0189 for θ. Also, for the goodness-of-fit statistics for the nonlinear regress, the SSE was $3.76e^{-07}$ and R-squared value was 1.

Figure 7 and Fig. 8 represent the ellipses that quantify the color fusion limit for each of the eight chromaticity points. All of the ellipses are plotted in the same scale. Table 2 summarizes the estimated parameter values and the goodness-of-fit statistics of the ellipses for the eight points. Figure 9 represents the overall results of the color fusion limit plotted on the CIE 1976 chromaticity diagram. For clarity, the plots are downscaled to one third of their actual lengths. In summary, the semi-minor axis, a, of the ellipses ranges from 0.0415 to 0.0923 in terms of the Euclidean distance in the u'v′ chromaticity diagram, whereas the semi-major axis, b, ranges from 0.0640 to 0.1560. The average of the a values is 0.0641 and the average of the b values is 0.1054.

The color fusion limit is not modeled as equal-sized circles in the standard uniform chromaticity diagram. It should be noted that the color fusion limit is modeled by a set of ellipses whose shapes and directions of rotation are similar to those of MacAdam ellipses for the just-noticeable differences of chromaticity [9,11]. For example, the ellipse for the No. 1 point has an elongated shape along the direction of the second and fourth quadrants in the u'v′ plane (see Fig. 7(a)). The ellipse for the No. 4 point has an oval shape with the major radius along the u′ axis (see Fig. 8(b)). The ellipse for the No. 8 point has an elongated shape along the v′ axis (see Fig. 8(f)). The ellipses of the other points also look similar in terms of their shape and direction of rotation. However, we cannot directly compare the two ellipses, as the observed points of the color fusion limit are different from those of the color difference; moreover, the MacAdam ellipses transformed to the u′v′ chromaticity diagram are not ellipses in a strict mathematical sense (their shapes closely resemble those of ellipses) [12].

#140993 - $15.00 USD Received 12 Jan 2011; revised 10 Mar 2011; accepted 21 Mar 2011; published 1 Apr 2011

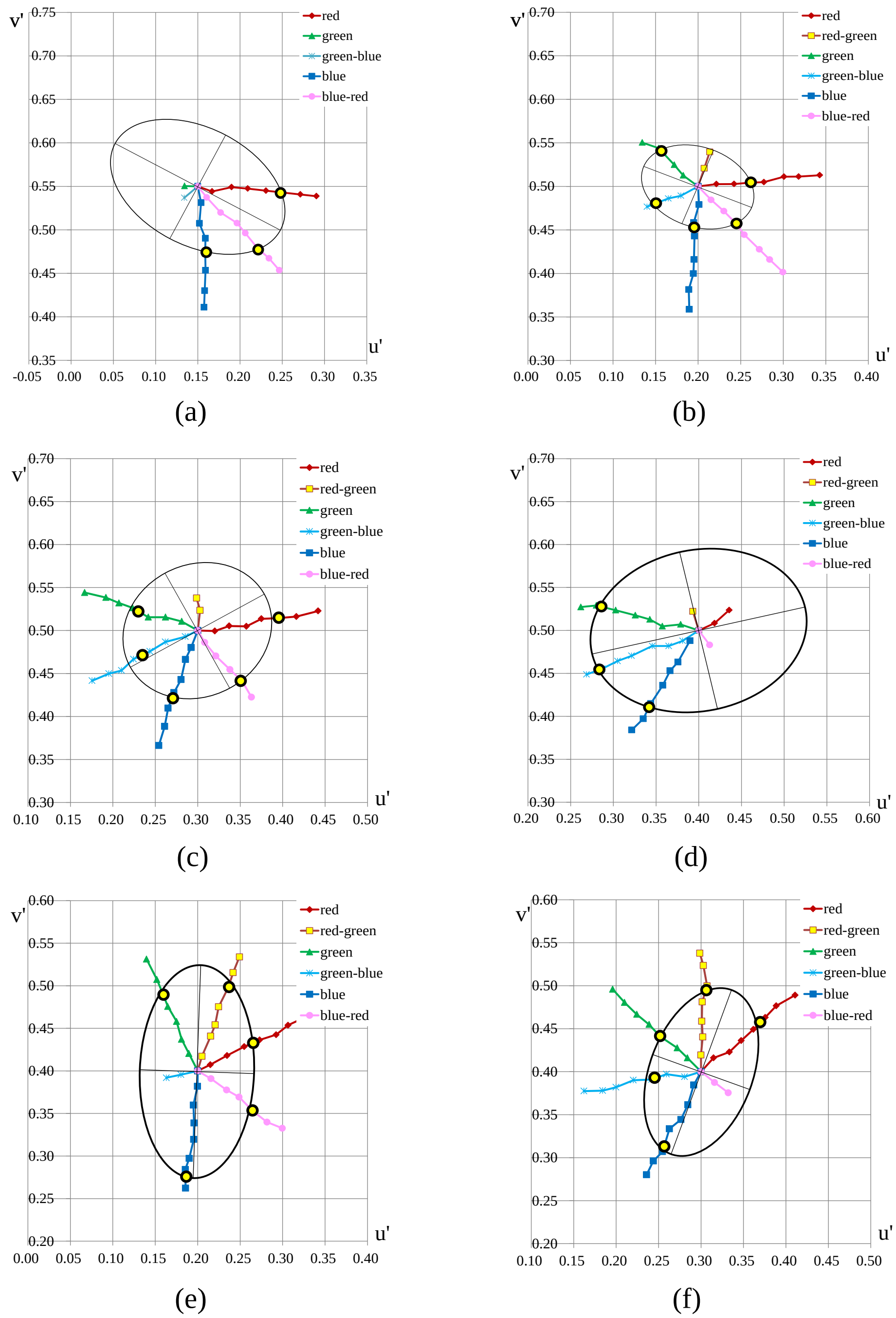

Fig. 7. Binocular color fusion limit for each of the chromaticity points in Fig. 2. The parameters of the ellipses were obtained by nonlinear regression. (a) No. 1 point (u´ = 0.15, v´ = 0.55), (b) No. 2 point (u´ = 0.2, v´ = 0.5), (c) No. 3 point (u´ = 0.3, v´ = 0.5), (d) No. 4 point (u´ = 0.4, v´ = 0.5), (e) No. 5 point (u´ = 0.2, v´ = 0.4), and (f) No. 6 point (u´ = 0.3, v´ = 0.4). The fusion limit along each line was marked.

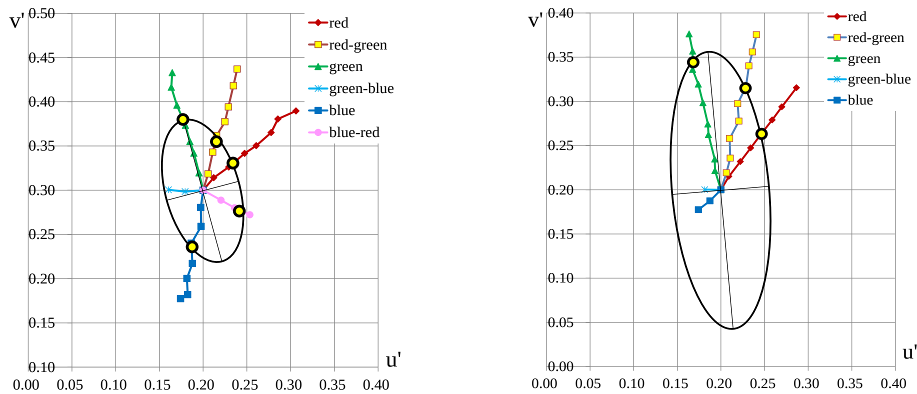

(a) (b)

Fig. 8. Binocular color fusion limit for each of the chromaticity points in Fig. 2. The parameters of the ellipses were obtained by nonlinear regression. (a) No. 7 point (u´ = 0.2, v´ = 0.3), and (b) No. 8 point (u´ = 0.2, v´ = 0.2). The fusion limit along each line was marked.

Table 2. Estimated Parameter Values and the Goodness-of-Fit Statistics of Ellipses for Each of the Eight Chromaticity Points.

Sample No.	Chromaticity point		Estimate			Std. Error			SSE	R-square
	u´	v´	*a*	*b*	*θ*(degree)	*a*	*b*	*θ*(degree)		
1	0.15	0.55	0.0707	0.1049	62.0273	0	0	0.0189	$3.76e^{-07}$	1.0000
2	0.2	0.5	0.0477	0.0640	–111.8408	0.0014	0.0017	3.3736	0.0276	0.9932
3	0.3	0.5	0.0772	0.0871	118.5364	0.0067	0.0067	29.7165	0.2563	0.9783
4	0.4	0.5	0.0923	0.1253	103.4114	0	0	0	$2.77e^{-31}$	1.0000
5	0.2	0.4	0.0653	0.1232	–1.5731	0.0016	0.0032	1.8604	0.0292	0.9988
6	0.3	0.4	0.0609	0.1014	–20.4477	0.0037	0.0064	5.2179	0.1640	0.9841
7	0.2	0.3	0.0415	0.0810	15.2235	0.0023	0.0048	4.8822	0.1219	0.9836
8	0.2	0.2	0.0569	0.1560	5.3398	0	0	0	$7.35e^{-31}$	1.0000

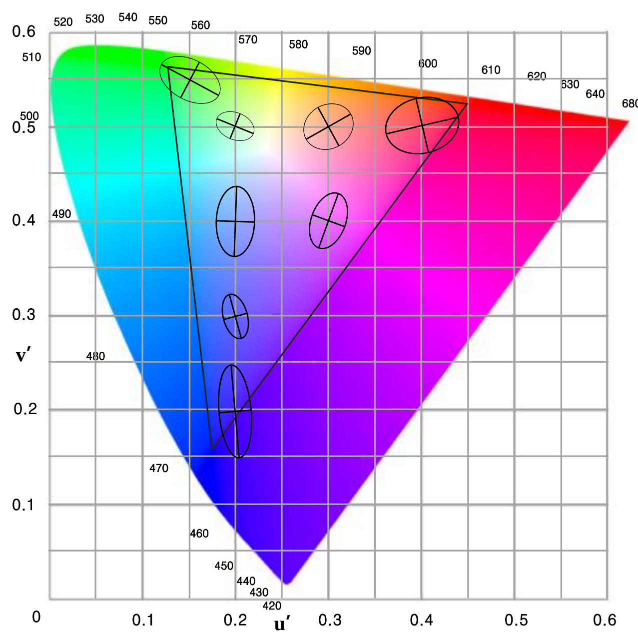

Fig. 9. Overall results of the color fusion limit plotted on the CIE 1976 chromaticity diagram. For clarity, the ellipses are downscaled to one third of their actual lengths.

#140993 - $15.00 USD Received 12 Jan 2011; revised 10 Mar 2011; accepted 21 Mar 2011; published 1 Apr 2011

To check the consistency of our measurement with the result of a previous study, we also compared our results with the results of a white point. Ikeda *et al.* [4] reported that the color fusion limit for a white point (u=0.1864, v=0.3196) was obtained in the form of a circle with a radius of about 0.0792 in the CIE 1960 uv chromaticity diagram. For the comparison, the color fusion limit was measured along the lines of the red and blue directions from the white point. The color fusion limits, as represented in the Euclidean distance from the white point in the CIE 1960 uv plane, were 0.0833 for the red direction and 0.0673 for the blue direction. Both values were close to Ikeda's result of 0.0792.

Furthermore, one of the present authors, YJ, made observations to confirm the above results of the color fusion limit obtained from DH's observations. As mentioned earlier, only four important chromaticity points were tested to avoid undue visual fatigue. The four points were the three points near the R, G, and B primaries (No. 1, No. 4, and No. 8) and one point near the center of the chromaticity diagram (No. 5). We observed that DH's curves did not significantly differ from those of YJ. The average differences of the color fusion limits, represented in the Euclidean distance in the u´v´ plane, were 0.0124 for the No. 1 point, 0.0023 for the No. 4 point, 0.0132 for the No. 5 point, and 0.0108 for the No. 8 point, respectively. The average difference of the color fusion limits for the four points was 0.0102 in terms of the u'v´ distance. The data for the two observers indicate that their color sensitivity and stereo vision are not different. In clinical tests, the two observers had normal color vision and normal stereo vision: Visual acuities for DH and YJ were 20/25 and 20/20, respectively, in the Snellen chart. Both had normal color vision according to the Ishihara test. In the Farnsworth-Munsell 100-hue arrangement test, the total error scores for DH and YJ were 7 and 0, respectively. A zero score indicates the perfect arrangement of colors, and a large total error score indicates a high number of color misplacements [13]. Both had very low score, that is, high color acuity. Moreover, both had stereo acuity of 40 seconds of arc in the Titmus stereo fly test.

In addition, a better fit may be searched for the observed psychometric functions instead of linear interpolation as in Figs. 5 and 6. To investigate the fitting of psychometric functions, we fitted the observed psychometric function with a logistic function [20]. In order to compare the difference between the use of linear interpolation and the fitting of a logistic function, we measured the Euclidean distance between the color fusion limits obtained by two methods. The average difference value of the color fusion limits was 0.0028 for all the eight chromaticity points. Consequently, the difference in the fitting results was not much to affect the measurement of color fusion limits.

4. Conclusions

Previous research investigated the binocular color fusion limit for spectral colors, represented as the wavelength difference. However, an investigation of the color fusion limit for non-spectral colors has not been done thus far. Hence, we conducted a quantitative investigation of the color fusion limit for non-spectral colors. The measurements were made at eight chromaticity points on the standard CIE 1976 chromaticity diagram. For the eight chromaticity points, the results of the color fusion limit were represented as a series of ellipses. The semi-minor axis of the ellipses ranged from 0.0415 to 0.0923 in the Euclidean distance in the u'v´ chromaticity diagram while the semi-major axis ranged from 0.0640 to 0.1560. The shapes and directions of rotation of the ellipses were similar to those of MacAdam ellipses for the just-noticeable differences of chromaticity.

We expect that our quantification of the color fusion limit will be utilized for various applications, such as an automatic stereo analyzer to guide content creators in the creation of visually comfortable stereoscopic contents, safety guidelines for watching 3DTV, and stereoscopic video quality metrics.

#140993 - $15.00 USD Received 12 Jan 2011; revised 10 Mar 2011; accepted 21 Mar 2011; published 1 Apr 2011

Appendix

Table 3. Stimuli and Percentages of Fused Perceptions for Binocular Color Fusion. p(%) Refers to the Percentage of Fused Perceptions.

right stimulus number	left stimulus number	u' (measured)	v' (measured)	luminance (measured, cd/m^2)	u'v' distance from right stimulus	p(%)	left stimulus number	u' (measured)	v' (measured)	luminance (measured, cd/m^2)	u'v' distance from right stimulus	p(%)
No. 1	1	0.1668	0.5441	10.62	0.0178	100	13	0.1588	0.4727	11.15	0.0778	50
	2	0.1899	0.5491	10.56	0.0399	100	14	0.1591	0.4534	11.03	0.0970	20
	3	0.2091	0.5474	10.16	0.0592	90	15	0.1581	0.4300	11.08	0.1203	0
	4	0.2307	0.5450	10.27	0.0809	80	16	0.1574	0.4110	11.11	0.1392	0
	5	0.2505	0.5429	10.83	0.1008	40	17	0.1605	0.5373	10.87	0.0165	100
	6	0.2714	0.5407	10.61	0.1218	0	18	0.1770	0.5199	10.87	0.0404	100
	7	0.2904	0.5387	10.47	0.1409	10	19	0.1964	0.5078	11.08	0.0627	100
	8	0.1343	0.5504	10.36	0.0157	100	21	0.2062	0.4963	11.07	0.0777	70
	9	0.1339	0.5368	10.53	0.0208	90	21	0.2204	0.4793	11.44	0.0998	50
	10	0.1539	0.5311	10.66	0.0193	100	22	0.2343	0.4673	11.63	0.1181	0
	11	0.1519	0.5074	10.90	0.0426	100	23	0.2465	0.4536	11.71	0.1364	0
	12	0.1590	0.4903	11.20	0.0604	70						
No. 2	1	0.2214	0.5026	11.20	0.0216	100	16	0.1399	0.4765	10.80	0.0645	0
	2	0.2422	0.5027	11.43	0.0423	90	17	0.2010	0.4790	11.24	0.0210	100
	3	0.2584	0.5041	11.40	0.0585	60	18	0.1948	0.4583	11.29	0.0420	70
	4	0.2773	0.5049	11.30	0.0775	10	19	0.1957	0.4428	11.41	0.0574	30
	5	0.3009	0.5111	11.39	0.1015	10	20	0.1951	0.4160	11.49	0.0841	0
	6	0.3181	0.5112	11.31	0.1186	0	21	0.1944	0.3998	11.62	0.1004	0
	7	0.3428	0.5128	11.23	0.1434	0	22	0.1890	0.3815	11.56	0.1190	0
	8	0.2072	0.5208	11.03	0.0220	100	23	0.1896	0.3587	11.45	0.1417	0
	9	0.2136	0.5396	10.93	0.0419	100	24	0.2152	0.4846	11.24	0.0216	90
	10	0.1825	0.5126	11.01	0.0216	100	25	0.2302	0.4716	11.62	0.0415	70
	11	0.1719	0.5248	10.94	0.0375	100	26	0.2440	0.4579	11.63	0.0609	50
	12	0.1537	0.5439	10.45	0.0638	40	27	0.2542	0.4445	11.68	0.0776	20
	13	0.1343	0.5504	10.36	0.0828	20	28	0.2719	0.4277	11.69	0.1020	0
	14	0.1797	0.4892	11.29	0.0230	100	29	0.2840	0.4160	11.52	0.1188	0
	15	0.1649	0.4861	11.16	0.0378	100	30	0.2996	0.4015	11.30	0.1401	0
No. 3	1	0.3201	0.4994	11.23	0.0201	100	19	0.2436	0.4757	11.66	0.0614	60
	2	0.3370	0.5053	11.18	0.0374	100	20	0.2243	0.4667	11.66	0.0827	30
	3	0.3573	0.5048	11.20	0.0575	80	21	0.2101	0.4535	11.50	0.1012	0
	4	0.3750	0.5136	11.33	0.0762	90	22	0.1952	0.4498	11.21	0.1162	0
	5	0.3952	0.5145	11.15	0.0963	50	23	0.1755	0.4416	11.15	0.1375	0
	6	0.4162	0.5162	11.14	0.1173	20	24	0.2921	0.4801	11.54	0.0214	100
	7	0.4418	0.5227	10.87	0.1436	10	25	0.2855	0.4663	11.62	0.0367	100
	8	0.3027	0.5235	11.25	0.0237	100	26	0.2803	0.4429	11.66	0.0604	70
	9	0.2986	0.5378	10.70	0.0378	100	27	0.2719	0.4277	11.69	0.0776	70
	10	0.2811	0.5106	11.29	0.0217	100	28	0.2650	0.4096	11.59	0.0969	10
	11	0.2620	0.5155	11.24	0.0410	100	29	0.2610	0.3884	11.59	0.1182	0
	12	0.2417	0.5155	11.36	0.0603	80	30	0.2541	0.3662	11.47	0.1415	10
	13	0.2232	0.5264	11.15	0.0812	30	31	0.3082	0.4862	11.35	0.0161	100
	14	0.2072	0.5320	11.07	0.0982	20	32	0.3213	0.4704	11.51	0.0365	100
	15	0.1918	0.5384	10.91	0.1148	0	33	0.3379	0.4547	11.35	0.0591	90
	16	0.1668	0.5441	10.62	0.1403	0	34	0.3524	0.4410	11.50	0.0789	50
	17	0.2853	0.4929	11.38	0.0163	90	35	0.3632	0.4226	11.35	0.0999	10
	18	0.2618	0.4867	11.52	0.0404	100						
No. 4	1	0.4185	0.5084	11.23	0.0203	100	14	0.3213	0.4704	11.51	0.0841	90
	2	0.4356	0.5236	11.02	0.0427	100	15	0.3049	0.4643	11.41	0.1016	80
	3	0.3931	0.5222	11.22	0.0232	100	16	0.2870	0.4554	11.53	0.1215	60
	4	0.3788	0.5070	11.23	0.0223	100	17	0.2685	0.4487	11.65	0.1412	0
	5	0.3573	0.5048	11.20	0.0430	100	18	0.3897	0.4880	11.24	0.0158	100
	6	0.3428	0.5128	11.23	0.0586	100	19	0.3756	0.4631	11.42	0.0442	100
	7	0.3257	0.5176	11.18	0.0764	100	20	0.3664	0.4530	11.34	0.0578	90
	8	0.3027	0.5235	11.25	0.1001	70	21	0.3578	0.4360	11.45	0.0767	80
	9	0.2801	0.5291	11.19	0.1234	40	22	0.3438	0.4148	11.43	0.1021	60
	10	0.2620	0.5272	11.16	0.1407	30	23	0.3350	0.3971	11.38	0.1217	10
	11	0.3811	0.4878	11.30	0.0225	100	24	0.3215	0.3840	11.33	0.1401	0
	12	0.3649	0.4818	11.45	0.0395	100	25	0.4128	0.4831	11.09	0.0212	90
	13	0.3455	0.4818	11.22	0.0575	100						

#140993 - $15.00 USD Received 12 Jan 2011; revised 10 Mar 2011; accepted 21 Mar 2011; published 1 Apr 2011

Table 4. Continued.

right stimulus number	left stimulus number	u' (measured)	v' (measured)	luminance (measured, cd/m^2)	u'v' distance from right stimulus	p(%)	left stimulus number	u' (measured)	v' (measured)	luminance (measured, cd/m^2)	u'v' distance from right stimulus	p(%)
No. 5	1	0.2149	0.4073	11.60	0.0166	100	19	0.1590	0.4903	11.20	0.0992	40
	2	0.2346	0.4181	11.78	0.0390	100	20	0.1519	0.5074	10.90	0.1177	30
	3	0.2548	0.4285	11.80	0.0618	70	21	0.1397	0.5313	10.45	0.1445	0
	4	0.2729	0.4364	11.74	0.0815	30	22	0.1803	0.3956	11.43	0.0202	100
	5	0.2924	0.4425	11.55	0.1017	10	23	0.1630	0.3920	11.18	0.0379	100
	6	0.3064	0.4537	11.35	0.1192	10	24	0.1997	0.3819	11.75	0.0181	100
	7	0.3272	0.4634	11.28	0.1421	0	25	0.1949	0.3599	11.44	0.0404	100
	8	0.2050	0.4172	11.50	0.0179	100	26	0.1957	0.3388	11.50	0.0614	100
	9	0.2153	0.4408	11.50	0.0436	90	27	0.1953	0.3196	11.53	0.0805	100
	10	0.2205	0.4541	11.50	0.0579	100	28	0.1900	0.2973	11.44	0.1032	90
	11	0.2246	0.4753	11.42	0.0792	60	29	0.1854	0.2842	11.37	0.1167	70
	12	0.2360	0.4980	11.47	0.1044	50	30	0.1857	0.2623	11.07	0.1384	30
	13	0.2417	0.5155	11.36	0.1228	0	31	0.2156	0.3909	11.62	0.0181	100
	14	0.2492	0.5339	11.30	0.1427	10	32	0.2341	0.3776	11.73	0.0408	100
	15	0.1896	0.4204	11.38	0.0229	100	33	0.2487	0.3693	11.51	0.0576	100
	16	0.1809	0.4372	11.33	0.0418	100	34	0.2648	0.3530	11.19	0.0801	40
	17	0.1751	0.4581	11.10	0.0632	100	35	0.2816	0.3399	11.18	0.1013	0
	18	0.1647	0.4757	11.02	0.0835	90	36	0.2996	0.3327	10.85	0.1202	0
No. 6	1	0.3147	0.4160	11.40	0.0217	100	20	0.2099	0.4805	11.40	0.1208	0
	2	0.3334	0.4229	11.43	0.0405	100	21	0.1959	0.4959	11.15	0.1415	0
	3	0.3473	0.4361	11.51	0.0595	100	22	0.2806	0.3941	11.40	0.0203	100
	4	0.3617	0.4492	11.35	0.0789	70	23	0.2592	0.3971	11.70	0.0409	80
	5	0.3756	0.4631	11.42	0.0985	40	24	0.2419	0.3909	11.79	0.0588	40
	6	0.3886	0.4766	11.24	0.1171	0	25	0.2202	0.3901	11.82	0.0804	0
	7	0.4108	0.4890	11.17	0.1421	0	26	0.1997	0.3819	11.75	0.1019	0
	8	0.2999	0.4195	11.41	0.0195	100	27	0.1841	0.3780	11.54	0.1180	0
	9	0.3020	0.4404	11.42	0.0404	100	28	0.1620	0.3775	11.16	0.1398	0
	10	0.3009	0.4587	11.40	0.0587	100	29	0.2914	0.3845	11.36	0.0177	100
	11	0.3014	0.4812	11.53	0.0812	80	30	0.2845	0.3615	11.21	0.0415	100
	12	0.3071	0.4998	11.44	0.1001	40	31	0.2763	0.3443	11.13	0.0605	100
	13	0.3027	0.5235	11.25	0.1235	20	32	0.2628	0.3336	11.20	0.0761	100
	14	0.2986	0.5378	10.70	0.1378	0	33	0.2546	0.3070	11.05	0.1035	20
	15	0.2840	0.4160	11.52	0.0226	100	34	0.2438	0.2962	11.04	0.1180	10
	16	0.2719	0.4277	11.69	0.0395	100	35	0.2359	0.2801	10.94	0.1360	0
	17	0.2522	0.4407	11.61	0.0628	60	36	0.3159	0.3875	11.35	0.0202	100
	18	0.2388	0.4549	11.76	0.0822	0	37	0.3321	0.3755	11.15	0.0404	90
	19	0.2243	0.4667	11.66	0.1009	0						
No. 7	1	0.2121	0.3141	11.40	0.0186	100	18	0.1798	0.3734	11.45	0.0761	30
	2	0.2293	0.3262	11.39	0.0393	70	19	0.1700	0.3961	11.33	0.1007	0
	3	0.2474	0.3416	11.33	0.0631	10	20	0.1636	0.4164	11.28	0.1220	0
	4	0.2607	0.3504	11.34	0.0789	0	21	0.1647	0.4329	11.01	0.1375	0
	5	0.2777	0.3651	11.28	0.1014	0	22	0.1794	0.2984	11.44	0.0207	100
	6	0.2855	0.3805	11.32	0.1174	0	23	0.1603	0.3005	11.12	0.0397	60
	7	0.3062	0.3896	11.44	0.1389	0	24	0.1973	0.2804	11.16	0.0198	100
	8	0.2057	0.3184	11.51	0.0193	90	25	0.1977	0.2591	10.91	0.0410	100
	9	0.2110	0.3430	11.65	0.0444	70	26	0.1865	0.2401	10.64	0.0614	60
	10	0.2154	0.3618	11.63	0.0637	30	27	0.1877	0.2171	10.27	0.0838	10
	11	0.2249	0.3774	11.80	0.0813	0	28	0.1815	0.2002	10.01	0.1015	0
	12	0.2289	0.3942	11.74	0.0985	0	29	0.1823	0.1819	9.33	0.1194	0
	13	0.2346	0.4181	11.78	0.1231	0	30	0.1742	0.1774	9.31	0.1253	0
	14	0.2389	0.4369	11.75	0.1423	0	31	0.2204	0.2887	11.19	0.0233	100
	15	0.1953	0.3196	11.53	0.0202	100	32	0.2359	0.2801	10.94	0.0410	60
	16	0.1895	0.3418	11.51	0.0431	80	33	0.2534	0.2722	10.32	0.0602	0
	17	0.1849	0.3550	11.44	0.0570	80						
No. 8	1	0.2091	0.2151	10.26	0.0176	100	16	0.2407	0.3753	11.63	0.1800	0
	2	0.2223	0.2319	10.10	0.0389	100	17	0.2452	0.3948	11.63	0.2000	0
	3	0.2341	0.2473	10.37	0.0583	80	18	0.1932	0.2216	10.35	0.0226	100
	4	0.2469	0.2640	10.42	0.0793	50	19	0.1929	0.2347	10.52	0.0354	100
	5	0.2588	0.2790	10.62	0.0985	30	20	0.1857	0.2623	11.07	0.0639	100
	6	0.2698	0.2938	10.53	0.1169	10	21	0.1851	0.2743	11.22	0.0758	100
	7	0.2866	0.3154	10.79	0.1443	0	22	0.1794	0.2984	11.44	0.1005	100
	8	0.2063	0.2192	10.11	0.0202	100	23	0.1741	0.3194	11.28	0.1222	90
	9	0.2107	0.2357	10.47	0.0373	100	24	0.1676	0.3360	11.24	0.1398	80
	10	0.2100	0.2579	10.75	0.0588	100	25	0.1676	0.3567	11.24	0.1600	10
	11	0.2206	0.2776	10.96	0.0803	90	26	0.1635	0.3763	11.24	0.1800	0
	12	0.2192	0.2974	11.28	0.0993	100	27	0.1815	0.2002	10.01	0.0185	100
	13	0.2286	0.3161	11.32	0.1196	50	28	0.1875	0.1875	9.49	0.0177	80
	14	0.2321	0.3401	11.63	0.1437	40	29	0.1742	0.1774	9.31	0.0343	60
	15	0.2362	0.3559	11.63	0.1600	20						

#140993 - $15.00 USD Received 12 Jan 2011; revised 10 Mar 2011; accepted 21 Mar 2011; published 1 Apr 2011

Acknowledgements

A male volunteer, Mr. DH Kim, participated in the observations. The authors acknowledge his interest and patience.

#140993 - $15.00 USD Received 12 Jan 2011; revised 10 Mar 2011; accepted 21 Mar 2011; published 1 Apr 2011